

Sensor and Simulation Notes

Note 389

25 November 1995

Brewster-Angle Interface Between Flat-Plate  
Conical Transmission Lines

Carl E. Baum  
Phillips Laboratory

Abstract

This paper considers a technique for launching fast, high-voltage transients on conical transmission lines in air as can be used for a pulse-radiating antenna (e.g., a TEM horn or a lens IRA). This technique uses another conical transmission line in a medium of higher dielectric strength and higher permittivity (e.g., transformer oil). These two conical transmission lines are joined at the dielectric surface and inclined to give a Brewster angle matching of the wave for the principal electric-field component. The interface is also curved to remove astigmatism from this single-surface lens.

CLEARED  
FOR PUBLIC RELEASE

*PD/PA 12-19-95*

PL 95 - 0996

## 1. Introduction

One kind of impulse radiating antenna (IRA) is a lens IRA consisting of a conical transmission line (TEM horn) with a lens near the horn aperture to focus the wave at infinity [2, 4, 6, 10, 11]. Whether or not one includes the final lens there is still the problem of launching a fast high-amplitude TEM wave on the conical transmission line from some high voltage pulser. Going back from the horn aperture toward the apex, the spacing of the plates (conductors) decreases until at some position one needs to be concerned about voltage breakdown. One can increase the dielectric strength by using gases such as SF<sub>6</sub>, or a medium such as transformer oil. In the latter case, one has a relative dielectric constant greater than air, giving a mismatch at the boundary of this medium.

This paper considers an approach to optimizing the launch of the spherical TEM wave on the conical transmission line in air (or other gas) from another conical transmission line in a dielectric medium with relative permittivity greater than one. The dielectric boundary between these two is designed to utilize the Brewster-angle phenomenon, but there are limitations due to more than one component (polarization) of the electric field in the TEM wave. The TEM waves, being spherical on the conical transmission lines, when matched on the dielectric surface also require some curvature of this surface for optimal matching.

## 2. Brewster-Angle Interface Between Two Finite-Width Parallel-Plate Waveguides

Our Starting point is the well-known Brewster-angle relationship for an E (or TM) plane wave (uniform, single polarization) passing with total transmission between two uniform isotropic dielectrics meeting at a surface  $S_B$ . As indicated in fig. 2.1, let us consider such a wave as bounded by two infinitely wide parallel-plate waveguides which, of course, have different spacings in the two media, and are parallel to the propagation direction and perpendicular to the electric field in each medium. Assume that the incident wave comes from the left side, giving the transmitted wave to the right (with horizontal propagation for later antenna consideration). The incident side has parameters designated by subscript  $i$ , and the transmitted side has parameters designated by subscript  $t$ . Both sides have the same permeability (taken as  $\mu_0$ ). Summarizing [3] we have

$$\begin{aligned}
 \epsilon_r &\equiv \frac{\epsilon_i}{\epsilon_t} \\
 \cot(\psi_{iB}) &= \epsilon_r^{\frac{1}{2}} = \tan(\psi_{tB}) \\
 \sin(\psi_{iB}) &= [\epsilon_r + 1]^{-\frac{1}{2}} = \cos(\psi_{tB}) \\
 \cos(\psi_{iB}) &= \left[ \frac{\epsilon_r}{\epsilon_r + 1} \right]^{\frac{1}{2}} = \sin(\psi_{tB}) \\
 \psi_{iB} + \psi_{tB} &= \frac{\pi}{2} \text{ (or } 90^\circ) \\
 h_i &= \cos(\psi_{iB}) h_s = \left[ \frac{\epsilon_r}{\epsilon_r + 1} \right]^{\frac{1}{2}} h_s \\
 h_t &= \cos(\psi_{tB}) h_s = [\epsilon_r + 1]^{-\frac{1}{2}} h_s \\
 \frac{h_i}{h_t} &= \epsilon_r^{\frac{1}{2}}
 \end{aligned} \tag{2.1}$$

For the common case of transformer oil or polyethylene we have [5]

$$\begin{aligned}
 \epsilon_r &\approx 2.26, \quad \epsilon_r^{\frac{1}{2}} \approx 1.503 \\
 \psi_{iB} &\approx 33.6^\circ \\
 \psi_{tB} &\approx 56.4^\circ
 \end{aligned} \tag{2.2}$$

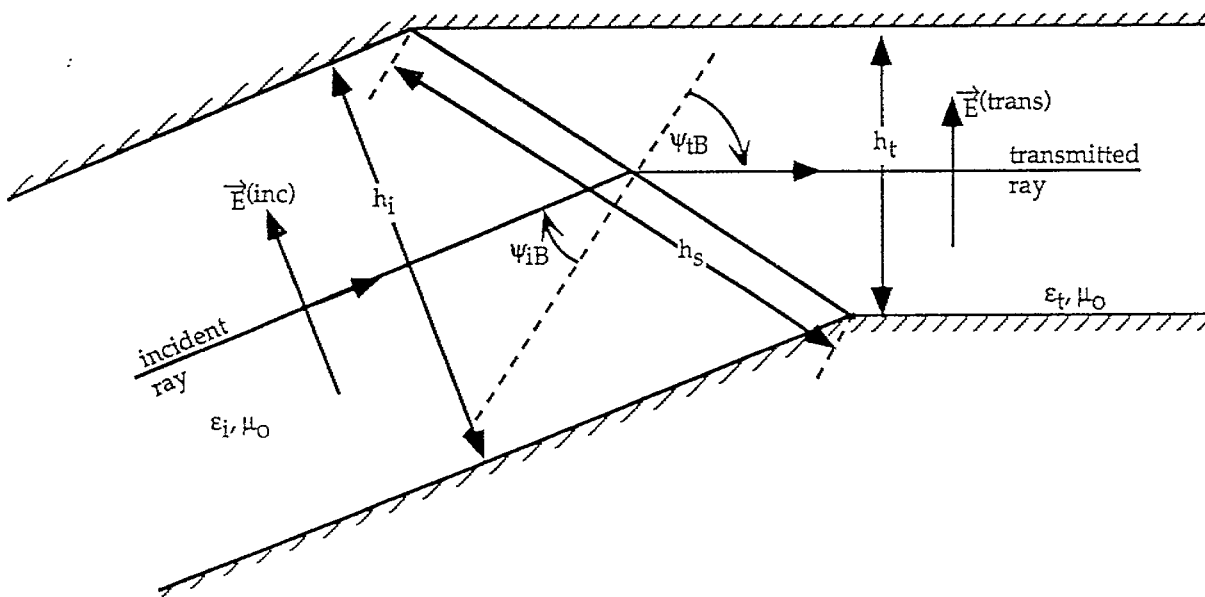


Fig. 2.1. Bend in Parallel-Plate Waveguide with Brewster-Angle Interface Between Two Dielectric Media

Note that we have assumed in fig. 2.1 that  $\epsilon_i > \epsilon_t$  so that the wave is propagating from some medium like oil out into air (or SF<sub>6</sub>, etc.). This is in preparation for the case that the plates are not parallel and the waves are expanding from left to right as spherical waves on conical plates in the two regions. The first region (subscript  $i$ ), then has much larger electric fields and needs a high dielectric strength medium such as oil before eventually transitioning through the Brewster interface S<sub>B</sub> and eventually radiating from an antenna.

Now let the plates have finite width. As in fig. 2.2, this can take the form of a plate of width  $w$  spaced a distance  $h$  above a large ground plane (say of width  $w + 2d$  with  $d \geq h$ ) for which the characteristic impedance (for the TEM mode) is approximately that of an infinitely wide ground plane. The characteristic impedance is written (for a free-space medium as on the transmitted side) as

$$Z_{ct} \equiv f_{gt} Z_0$$

$$Z_0 = \left[ \frac{\mu_0}{\epsilon_0} \right]^{\frac{1}{2}} = \mu_0 c \approx 376.73 \Omega \text{ (wave impedance of free space)}$$
(2.3)

From [1] we have the two cases for comparison

1.  $\frac{w_t}{h_t} = 1$  ,  $\frac{d_t}{h_t} = \infty$  ,  $f_{gt} \approx 0.336$  ,  $Z_{ct} \approx 127 \Omega$
2.  $\frac{w_t}{h_t} = 1$  ,  $\frac{d_t}{h_t} = 1$  ,  $f_{gt} \approx 0.364$  ,  $Z_{ct} \approx 137 \Omega$

(2.4)

which gives about an 8% increase for the finite-width ground plane. Note in fig. 2.2, that while our calculations are for a finite-width plate over a wide ground plane, as appropriate for the asymmetrical TEM horn in [6], they can also apply to a symmetrical case by considering the image at a distance  $h$  on the opposite side of the ground plane.

For continuity of the top plate through the Brewster interface S<sub>B</sub> one can set the two widths there as the same, i.e.,

$$w_i = w_t$$
(2.5)

This is not a necessary constraint, but it does reduce the discontinuity in the top plate, thereby reducing the electrical-breakdown problem for large electric fields (high voltage and high power) in the incident TEM wave. One consequence of this is the discontinuity in the characteristic impedance since

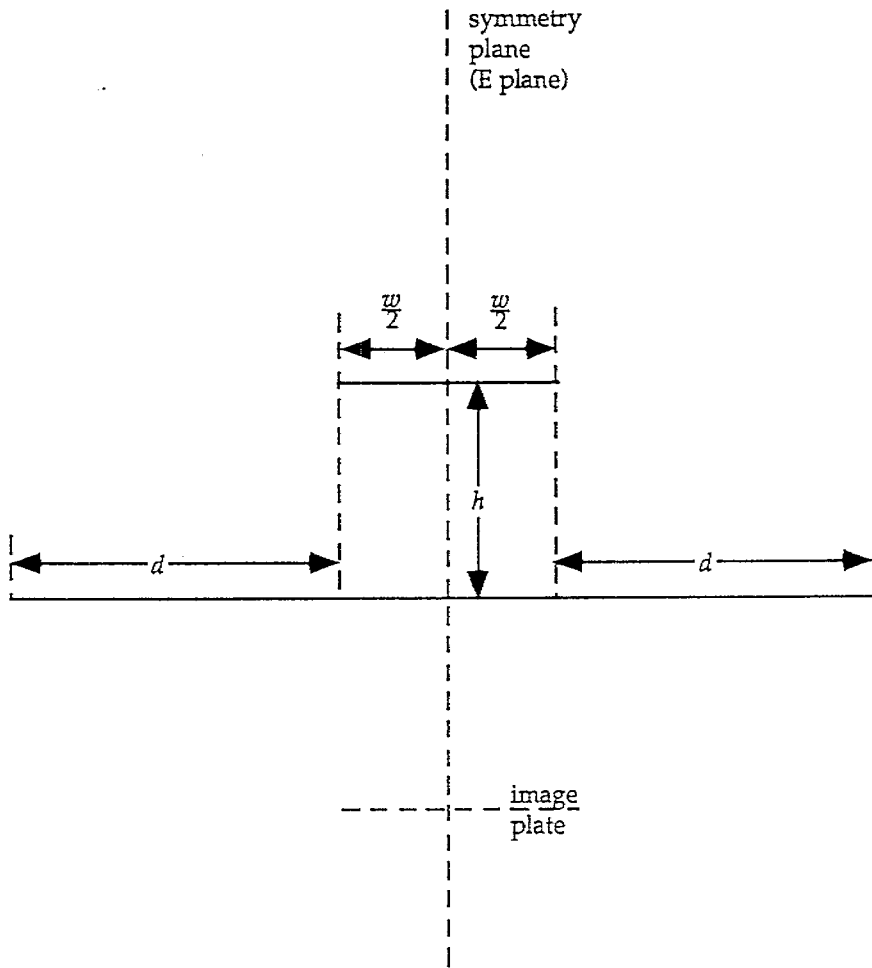


Fig. 2.2. Cross Section of Two-Parallel-Plate TEM Waveguide with at Least One Plate of Finite Width

$$h_i = \frac{1}{\epsilon_r^2} h_t \approx 1.503 h_t \quad (2.6)$$

implying for our example

$$\frac{w_i}{h_i} = \frac{1}{\epsilon_r^2} \frac{w_t}{h_t}, \quad Z_{ci} = \frac{1}{\epsilon_r^2} f_{gi} Z_o \quad (2.7)$$

$$f_{gi} \approx 0.401, \quad Z_{ci} \approx 100 \Omega \text{ for } \frac{d_i}{h_i} = \infty$$

which is about a 21% decrease in the characteristic impedance and which represents about a 0.1 reflection and a 1.1 transmission coefficient (voltage). If the plates were all infinitely wide the match would be exact. The characteristic-impedance discontinuity is associated with the fact that the Brewster-angle matching is associated only with the "vertical" electric field (perpendicular to the plates), and there are significant "horizontal" electric fields (parallel to the plates) which do not perfectly match through the Brewster interface. Note that a larger  $w_t/h_t$  (giving larger  $w_i/h_i$ ) implies a closer match in the characteristic impedances.

### 3. Antenna Aperture at Truncation of Second Parallel-Plate Waveguide

Consider now that the second parallel-plate waveguide (transmitted-wave section) continues to some aperture plane  $S_a$  where the waveguide is truncated, this aperture plane being perpendicular to the direction of propagation (and thereby to the waveguide conductors as well). Then the diagram in fig. 2.2 applies to the aperture plane, and a subscript  $a$  can be used to designate parameters at the aperture plane.

For the moment, with  $w_a = w_t$  and  $h_a = h_t$ , the early-time (or high-frequency) fields arrive at  $S_a$  following optical principles and thereby arrive all at the same time (or same phase) due to the plane-wave character of the fields. Note that this applies only over the portion of  $S_a$  illuminated in this sense by the fields from  $S_B$ , depending on how far the dielectric medium (illuminated side) extends beyond the top and sides of the top plate. Within this restriction we have the radiated far field on boresight is [2, 10]

$$\begin{aligned}\vec{E}_t(\vec{r}, t) &= \frac{1}{2\pi r} \frac{\partial}{\partial t} \int_{S_a} \vec{E}_t(\vec{r}', t_r) dS' \\ &\equiv \frac{A_a}{2\pi r} \frac{\partial}{\partial t} \vec{E}_{t_{avg}}(\vec{r}', t_r) dS' \\ A_a &\equiv \text{aperture area for significant fields on } S_a \\ r &\equiv \text{distance to observer on boresight} \\ c &\approx 2.998 \times 10^8 \frac{m}{s} \text{ (speed of light)} \\ t_r &\equiv t - \frac{r}{c} \equiv \text{retarded time} \\ \vec{E}_t(\vec{r}_s, t) &\equiv \text{tangential part of electric field on } S_a\end{aligned}\tag{3.1}$$

So a fast-rising field (simultaneously on  $S_a$ ) modeled as a step function produces a narrow impulse (approximate delta function) on boresight in the far field.

Now consider the integral in (3.1) and note the vertical symmetry plane in fig. 2.2. The fields are symmetric [12] with respect to this plane. The horizontal components of the electric field then contribute zero to this integral. The reflection of the horizontal components at the Brewster interface  $S_B$  then does not affect this integral (in the optical approximation, i.e., at early retarded time). The vertical components, being perfectly transmitted through  $S_B$  (early-time sense), are what contributes to the integral. Thus, for the early-time impulsive part of the far field, the transmission of the incident TEM wave through  $S_B$  can be regarded as though it were perfect.

#### 4. Replacement of Parallel-Plate Waveguides by Flat-Plate Conical Waveguides

The next step is to change the parallel-plate waveguides (finite top-plate width) into flat-plate conical waveguides as indicated in fig. 4.1 and discussed in [6]. For small inclination angles between the top plates and the two parts of the bent wide ground plane, the spherical TEM modes on the two conical transmission lines can be approximated by the TEM plane waves previously discussed. For wavelengths on the incident side of  $S_B$  large compared to  $w_i$  and  $h_i$ , a flat interface surface  $S_B$  will not be significant in that it does not perfectly match the spherical wavelengths on the two sides of the boundary; this is the transmission-line approximation.

For a better match for high frequencies or early time on the wavefront one can curve  $S_B$  so as to make the wave emerging from  $S_B$  appear to be a spherical wave with a virtual focus at the virtual apex of the conical transmission line (TEM horn) to the right of  $S_B$  in fig. 4.1. The virtual apex is to the left of  $S_B$ . If we have some central transmitted ray of interest (taken as horizontal in fig. 4.1), it is this continuation to the left of  $S_B$  as a virtual ray on which the virtual apex lies.

One can calculate the path of every ray passing from the source on the incident side to the transmitted side and force all of these to extrapolate to the left to a common point (the virtual focus or apex), and thereby determine the detailed shape of  $S_B$ . Some of this has been done in [7]. For present purposes, let us consider an approximate solution for  $S_B$  as a curved surface by considering the rays near the central ray.

Keep the E plane as a symmetry plane (fig. 2.2) for  $S_B$ . Then this E plane contains the central ray on both sides of  $S_B$  and the virtual ray to the left of  $S_B$  in fig. 4.1. Note that the E plane intersects  $S_B$  perpendicularly and contains the normal to  $S_B$  at the intersection with the central ray. Take another plane which we can call the H plane (referenced to  $S_B$ ) which is perpendicular to the E plane and also contains this same surface normal. Locally the H plane is also perpendicular to  $S_B$ .

In optics such a single refracting surface is referred to (in general) as *astigmatic* (from "a" meaning non and "stigma" meaning mark or focal point in this context). Considering a doubly curved surface in fig. 4.2, we have the relation of the angles for the central ray (with respect to the normal to some general surface S) as

$$\frac{1}{\epsilon_f^2} \sin(\psi_i) = \sin(\psi_t) \quad (4.1)$$

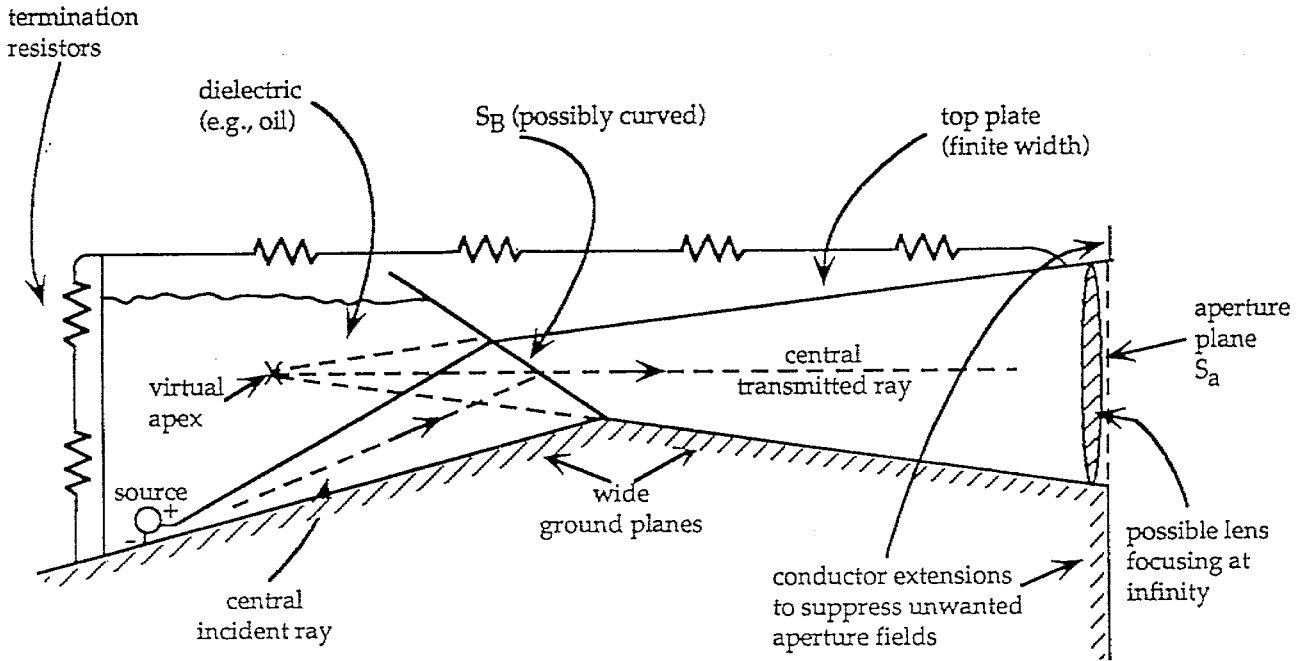
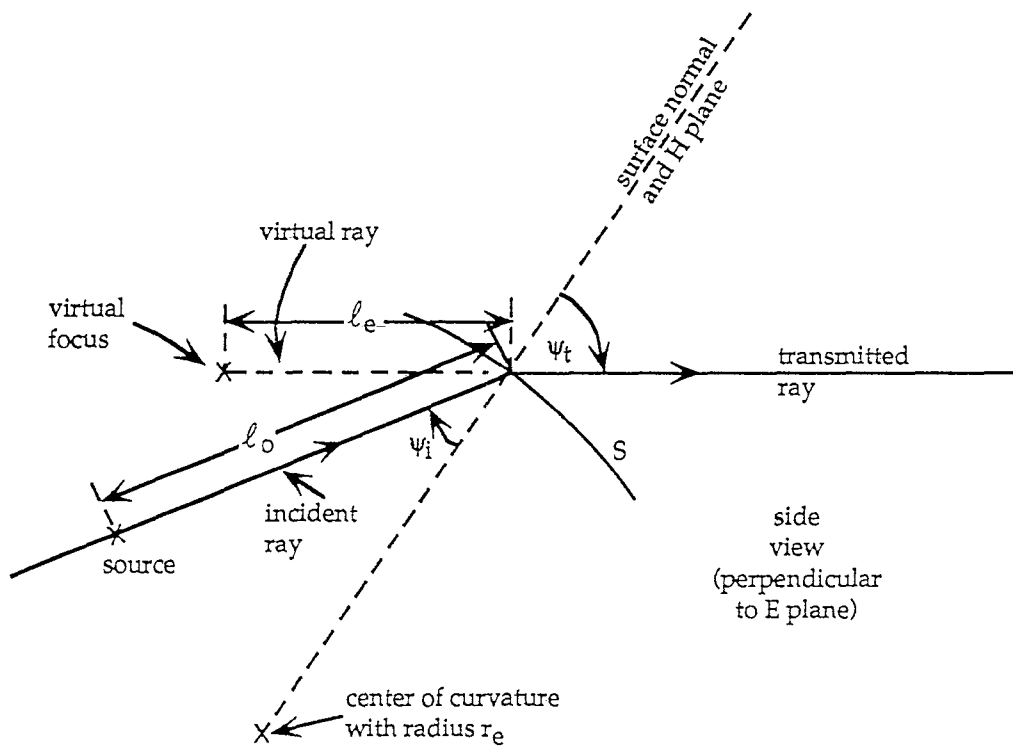
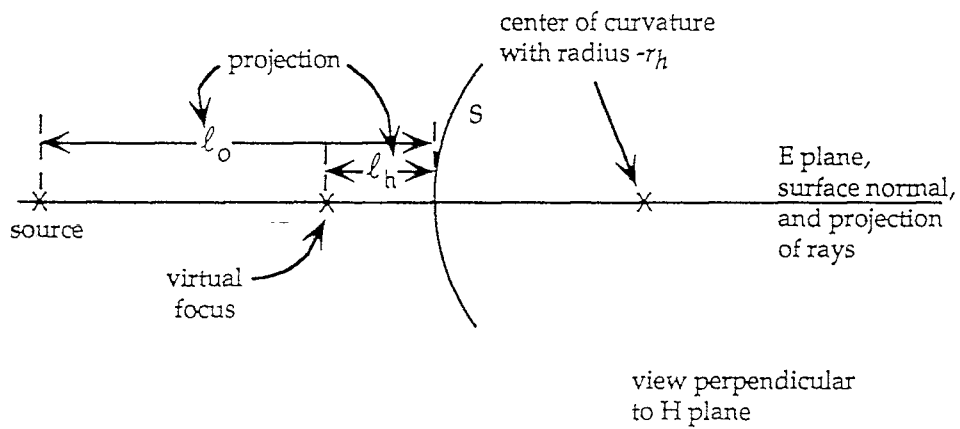


Fig. 4.1. Replacement of Top Plate by Flat-Plate Cones with Small Angle of Inclination with Respect to Wide Ground Plane



A. E-plane virtual apex (focus)



B. H-plane virtual apex (focus)

Fig. 4.2. Astigmatic Virtual Foci for E-Plane and H-Plane Rays

This is later applied to the case of the Brewster angle.

As in fig. 4.2A, the side view of the E plane shows S curved with a local radius of curvature  $r_e$  (centered to the left of S on the surface normal). In optics this E plane is also referred to as the *tangential* or *meridional* plane. The corresponding E plane focus (for E-plane rays) is a distance  $\ell_e$  to the left of S on the continuation of the transmitted ray giving a virtual focus). These are related by [8, 9]

$$\frac{1}{\epsilon_r^2} \frac{\cos^2(\psi_i)}{\ell_o} - \frac{\cos^2(\psi_t)}{\ell_e} = \frac{1}{\epsilon_r^2} \frac{\cos(\psi_i) - \cos(\psi_t)}{r_e} \quad (4.2)$$

where  $\ell_o$  is the distance of the source from S (along the incident ray).

Figure 4.2B shows a top view, normal to the H plane and giving the intersection of S with the H plane with radius of curvature  $r_h$ . Illustrated as a negative  $r_h$ , the center of curvature lies to the right of S. The surface normal lies in this plane but the rays of concern do not. In optics, this H plane is also referred to as the *sagittal* plane. The corresponding H-plane focus (for rays meeting the H plane at S) is a distance  $\ell_h$  to the left of S (virtual focus as before). These are related by [8, 9]

$$\frac{1}{\epsilon_r^2} \frac{1}{\ell_o} - \frac{1}{\ell_h} = \frac{1}{\epsilon_r^2} \frac{\cos(\psi_i) - \cos(\psi_t)}{r_h} \quad (4.3)$$

In general,  $\ell_e$  and  $\ell_h$  are different and  $\ell_h - \ell_e$  is called the *astigmatic difference*. For a given  $\psi_i$  (and hence  $\psi_t$ ),  $r_e$  and  $r_h$  can be adjusted to minimize this difference. Note that if S is flat ( $r_e = r_h = \infty$ ) this difference is zero for finite, non-zero  $\ell_o$  only if  $\psi_i = \psi_t = 0$ , i.e., normal incidence. For non-normal incidence S needs to be carved to remove the astigmatism (i.e., to make a *stigmatic lens*).

Specializing the results to the Brewster-angle case, let S be  $S_B$  which is now, in general, curved but with the central ray described by (2.1). Then the E-plane focus is given by

$$\begin{aligned} \frac{3}{\epsilon_r^2} \frac{1}{\ell_o} - \frac{1}{\ell_e} &= \frac{1}{[\epsilon_r + 1]2} \frac{[\epsilon_r - 1]}{r_e} \\ \frac{\ell_e}{\ell_o} &= \left\{ \frac{3}{\epsilon_r^2} - \frac{1}{[\epsilon_r + 1]2} \frac{[\epsilon_r - 1]}{r_e} \right\}^{-1} \end{aligned} \quad (4.4)$$

and the H-plane focus is given by

$$\frac{1}{\frac{\epsilon_r^2}{\ell_0} - \frac{1}{\ell_h}} = \frac{[\epsilon_r + 1]^{-\frac{1}{2}} [\epsilon_r - 1]}{r_h} \quad (4.5)$$

$$\frac{\ell_h}{\ell_0} = \left\{ \epsilon_r^2 - [\epsilon_r + 1]^{-\frac{1}{2}} [\epsilon_r - 1] \frac{\ell_0}{r_h} \right\}^{-1}$$

For flat  $S_B$ , these reduce to

$$\frac{\ell_e}{\ell_0} = \epsilon_r^{-\frac{3}{2}}, \quad \frac{\ell_h}{\ell_0} = \epsilon_r^{-\frac{1}{2}} \quad (4.6)$$

so that for transformer oil and/or polyethylene on the incident side we have (from (2.2))

$$\frac{\ell_0}{\ell_e} = 3.40, \quad \frac{\ell_0}{\ell_h} = 1.503 \quad (4.7)$$

$$\frac{\ell_e}{\ell_0} = 0.294, \quad \frac{\ell_h}{\ell_0} = 0.665$$

So, for flat  $S_B$ , the length of the incident conical transmission line is considerably larger than that of the image portion of the transmitted conical transmission line. Said another way, flat  $S_B$  implies a significantly larger angle of divergence for the transmitted conical transmission line as compared to the incident conical transmission line. Furthermore, for  $\ell_0 \neq \infty$ , the lens is astigmatic so that a unique apex for the transmitted conical transmission line cannot be defined. One may choose some length between  $\ell_e$  and  $\ell_h$  for the conical apex as a compromise for constructing the transmitted conical transmission line, and accept the degraded performance implied by the astigmatism.

Another special case of interest is for a singly curved  $S_B$  (cylindrical surface). For this we need to set  $r_h$  or  $r_e$  (but not both) equal to infinity. The remaining curvature can then be computed to make  $\ell_h = \ell_e$ . Choosing  $S_B$  to be flat in the H plane we have

$$r_h = \infty, \quad \frac{\ell_h}{\ell_0} = \epsilon_r^{-\frac{1}{2}} \quad (4.8)$$

Equating the two foci then gives from (4.4)

$\approx$

$$\frac{r_e}{l_o} = \left[ \frac{\epsilon_r + 1}{\epsilon_r} \right]^{\frac{1}{2}} = \sec(\psi_{iB}) = \csc(\psi_{tB}) \quad (4.9)$$

$$\frac{r_e}{l_e} = \frac{r_e}{l_h} = [\epsilon_r + 1]^{\frac{1}{2}} = \csc(\psi_{iB}) = \sec(\psi_{tB})$$

For transformer oil and/or polyethylene on the incident side we then have

$$\frac{l_n}{l_o} = \frac{l_e}{l_o} = 0.665 \quad , \quad \frac{l_o}{l_h} = \frac{l_o}{l_e} = 1.503 \quad (4.10)$$

$$\frac{r_e}{l_o} \approx 1.20 \quad , \quad \frac{r_e}{l_e} = \frac{r_e}{l_h} \approx 0.665$$

All these ratios are conveniently within a factor of two from unity. This case is roughly illustrated in fig. 4.2A.

An alternate choice for a singly curved  $S_B$  is to choose

$$r_e = \infty \quad , \quad \frac{l_e}{l_o} = \epsilon_r^{-\frac{3}{2}} \quad (4.11)$$

Equating the two foci then gives

$$\frac{r_h}{l_o} = - \epsilon_r^{-\frac{1}{2}} [\epsilon_r + 1]^{\frac{1}{2}} = - \sin(\psi_{iB}) \tan(\psi_{iB}) = - \cos(\psi_{tB}) \cot(\psi_{tB}) \quad (4.12)$$

$$\frac{r_h}{l_e} = \frac{r_h}{l_h} = - \epsilon_r [\epsilon_r + 1]^{\frac{1}{2}} = - \cos(\psi_{iB}) \cot(\psi_{iB}) = - \sin(\psi_{tB}) \tan(\psi_{tB})$$

Note the minus sign implying a negative  $r_h$  which is interpreted as a center of curvature to the right of  $S_B$  (transmitted side). For transformer oil and/or polyethylene on the incident side we then have

$$\frac{l_e}{l_o} = \frac{l_e}{l_o} \approx 0.294 \quad , \quad \frac{l_o}{l_e} = \frac{l_o}{l_h} \approx 3.40 \quad (4.13)$$

$$\frac{r_h}{l_o} \approx -0.368 \quad , \quad \frac{r_h}{l_e} = \frac{r_h}{l_h} \approx -1.25$$

The choice of  $r_e = \infty$ , then results in a larger deviation of  $l_o$  from  $l_e = l_h$  than the previous choice of  $r_h = \infty$ . This case is roughly illustrated in fig. 4.2B.

## 5. Concluding Remarks

The matching of the spherical TEM waves at the Brewster interface  $S_B$  is then not perfect. There is some mismatch due to the portion of the electric field with polarization not suited for the Brewster angle. Of course, this interface  $S_B$  introduces a bend at the connection of the two conical transmission lines. As we have seen  $S_B$  needs to be curved to give the wave leaving from  $S_B$  a unique virtual focus which can be taken as the apex of the output conical transmission line. However, it is possible to make  $S_B$  singly curved and still achieve this unique virtual focus. Note that in this paper we have assumed that the angles of divergence of the conical transmission lines are sufficiently small that the usual lens formulas involving a central ray apply to a good approximation over the entire lens surface.

This Brewster matching is, of course, only part of the design considerations for a fast, high-voltage TEM horn. There is the lens to be added near the horn aperture to focus the fields at infinity. Furthermore, as discussed in [6], there is the resistive termination for the low-frequency load to be seen by the high voltage pulser, and for the optimization of the low-frequency radiation by optimal combination of electric and magnetic dipole moments. There is still the design of the pulser and its matching to the conical transmission line on the incident side of  $S_B$  to consider. There are issues of impedance matching from the pulser and associated impedance transformation (e.g., a transmission-line transformer) to consider, but these are beyond the scope of this paper.

## References

1. G. W. Carlisle, Impedance and Fields of Two Parallel Plates of Unequal Breadths, *Sensor and Simulation Note 90*, July 1969.
2. C. E. Baum, Radiation of Impulse-Like Transient Fields, *Sensor and Simulation Note 321*, November 1989.
3. C. E. Baum, Wedge Dielectric Lenses for TEM Waves Between Parallel Plates, *Sensor and Simulation Note 332*, September 1991.
4. E. G. Farr and C. E. Baum, A Simple Model of Small-Angle TEM Horns, *Sensor and Simulation Note 340*, May 1992.
5. C. E. Baum, J. J. Sadler, and A. P. Stone, A Uniform Dielectric Lens for Launching a Spherical Wave into a Paraboloidal Reflector, *Sensor and Simulation Note 360*, July 1993.
6. C. E. Baum, Low-Frequency-Compensated TEM Horn, *Sensor and Simulation Note 377*, January 1995.
7. J. D. Shipman, Jr., Oil-Gas Brewster-Angle Interface for a Spherical Wavefront, *Circuit and Electromagnetic System Design Note 20*, November 1967.
8. G. S. Monk, *Light, Principles and Experiments*, McGraw Hill, 1937.
9. F. A. Jenkins and H. E. White, *Fundamentals of Optics, 4th Ed.*, McGraw Hill, 1976.
10. C. E. Baum and E. G. Farr, Impulse Radiating Antennas, pp. 139-147, in H. Bertoni et al (eds.), *Ultra-Wideband, Short-Pulse Electromagnetics*, Plenum Press, 1993.
11. E. G. Farr, C. E. Baum, and C. J. Buchenauer, Impulse Radiating Antennas, Part II, pp. 159-170, in L. Carin and L. B. Felsen (eds.), *Ultra-Wideband, Short-Pulse Electromagnetics 2*, Plenum Press, 1995.
12. C. E. Baum and H. N. Kritikos, Symmetry in Electromagnetics, Ch. 1, pp. 1-90, in C. E. Baum and H. N. Kritikos (eds.), *Electromagnetic Symmetry*, Taylor & Francis, 1995.